Lithium-Lead/Water Interactions and Associated Structural Responses in a Fusion System

S.W. Lomperski, M.L. Corradini

February 1988

UWFDM-759

FUSION TECHNOLOGY INSTITUTE

UNIVERSITY OF WISCONSIN

MADISON WISCONSIN

Lithium-Lead/Water Interactions and Associated Structural Responses in a Fusion System

S.W. Lomperski, M.L. Corradini

Fusion Technology Institute
University of Wisconsin
1500 Engineering Drive
Madison, WI 53706

http://fti.neep.wisc.edu

February 1988

UWFDM-759

LITHIUM-LEAD/WATER INTERACTIONS AND ASSOCIATED STRUCTURAL RESPONSES IN A FUSION SYSTEM

S.W. Lomperski and M.L. Corradini

Fusion Technology Institute
Nuclear Engineering Department
University of Wisconsin-Madison
1500 Johnson Drive
Madison, WI 53706

February 1988

UWFDM-759

ABSTRACT

Tube ruptures in steam generators containing lithium-lead are expected to result in temperature and pressure transients due to the reaction of lithium with water. The temperature and pressure transients provided by the Metal Water Interactions (MWI) computer code are utilized to determine subsequent effects upon the steam generator components. A second computer code, the Advanced Thermal Hydraulic Energy Network Analyzer (ATHENA), was used in an attempt to compare the temperature and pressure transients predicted by the first. ATHENA is not designed to model liquid-metal chemical reactions and so it compared unfavorably with the MWI results. For stress analysis, three cases were considered: loading on a double-wall steam tube adjacent to the broken tube; loading on the steam generator shell for tube breaks near the center of the tube array; and loading on the shell for breaks at the edge of the tube array. Only in the last case was it found that stresses could exceed the yield stress of the structural material (HT-9 was chosen).

Heat generated by the lithium-water reaction may have deleterious effects upon steam tubes surrounding the break. Due to the brief period of the pressure transient, no significant heating of the tube will take place before the intial pressure wave passes. The structural strength of the steam tube does not degrade appreciably during the transient. Long after the tube break, the continuing lithium-water reaction can heat the outer tube wall so that it is able to safely bear only a fraction of the tube to shell side pressure drop.

INTRODUCTION

Various heat transfer mediums have been proposed for future fusion systems. Unlike fission power reactors, fusion designs often require the coolant to serve the dual purpose of removing heat from the fusion reaction and breeding additional fuel (this is the case for systems that utilize the deuterium-tritium reaction). Lithium, and a number of its alloys, possess many desirable properties for the performance of these tasks. Unfortunately, pure lithium is highly reactive with numerous substances, most notably water. This has prompted more careful study of lithium alloys such as lithium-lead ($Li_{17}Pb_{83}$). Though lithium-lead is considerably less reactive than pure lithium it may pose a danger when the molten form is mixed with steam or water [1]. The possibility of a reaction with an explosive nature is of great concern, especially when a fusion system component carries both lithium-lead and water; e.g. the steam generator.

Among the potentially serious safety hazards associated with a steam generator employing lithium-lead as a shell side heat transfer medium is a steam tube rupture. The large pressure differential between the water and liquid metal forces water into the lithium-lead that surrounds the break, resulting in a shell side pressure increase. A chemical reaction between the lithium and water begins almost immediately and local temperatures sharply elevate. This excessive heat and pressure may precipitate a breach in adjacent steam tubes, conceivably producing a chain reaction of failures and causing extensive damage to the interior of the steam generator. It is of interest to examine the effects of the transients upon the structural integrity of various components of the steam generator. In particular, the effects of pressure waves and temperature transients upon the outer shell and steam tubes will be investigated.

Two computer codes are used to independently obtain the system pressure response near the steam tube break. The Metal-Water Interactions (MWI) code developed at the University of Wisconsin [2,3] is a lumped parameter model that is designed specifically for this type of event. The Advanced Thermal Hydraulic Energy Network Analyzer (ATHENA) code from the Idaho National Engineering Laboratory [4] is a one-dimensional transient analysis code designed to simulate advanced thermal hydraulic systems. ATHENA, derived mainly from RELAP5 [5], is quite general and provides for the use of a wide variety of fluids. However, the inability of this code to mix two dissimilar fluids leads one to expect difficulties in modeling this type of transient.

Once we are supplied with a pressure history, our attention turns to modelling the stresses on the steam generator. Its complex structure was simplified so that stresses and natural frequencies of vibration could be calculated with analytical models. Steam tubes and the steam generator outer shell are the components to be examined. Both are considered to be isolated, clamped cylinders.

It was deemed impractical to treat the general case of a tube rupture at any position in the steam generator. Two limiting cases are investigated: a tube rupture in the center of the steam generator and a rupture at the outside edge of the tube array.

METAL-WATER INTERACTION MODEL

The scenario of interest is a sudden and complete coolant tube rupture within a steam generator which results in high pressure injection of water into molten lithium-lead. The models for coolant injection and structural analysis are considered for the Westinghouse large scale breeder reactor steam generator shown in Fig. 1 [6]. Figure 2 is a simplified sketch of the tube rupture [7]. The MWI model generates a temperature and pressure response in the vicinity of the tube break by making the following assumptions:

- Complete mixing and reaction of water with lithium-lead creating a homogeneous and spherical 'reaction zone' around the tube break. The reaction zone is the volume containing the mixture of lithium-lead, steam, and reaction products. This volume is in thermal equilibrium and may grow in time.
- There is no back flow through the broken steam tube.
- The flow rate of water into the reaction zone is modeled by a one dimensional homogeneous equilibrium model for critical flow.
- The reactants remain in the reaction zone during the brief time of interest.
- The pressure increase in the shell side of the steam generator suspends the flow of lithium-lead.
- The initial pressure of the reactants is 17.0 MPa for the water and 0.17 MPa for the lithium-lead. The initial liquid metal temperature is taken to be 673 K and the water is 648 K.

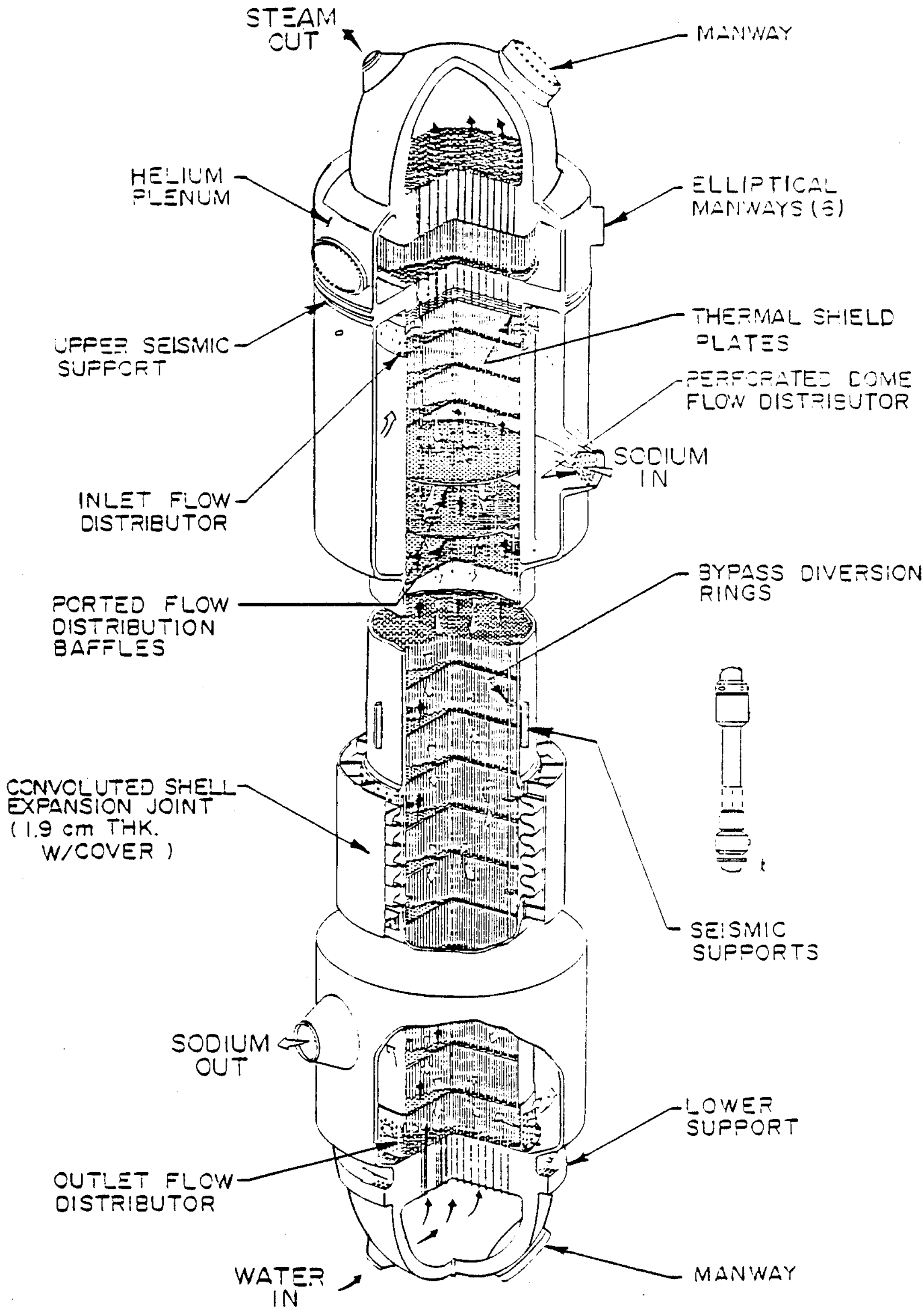

Fig. 1. Westinghouse large scale breeder reactor steam generator.

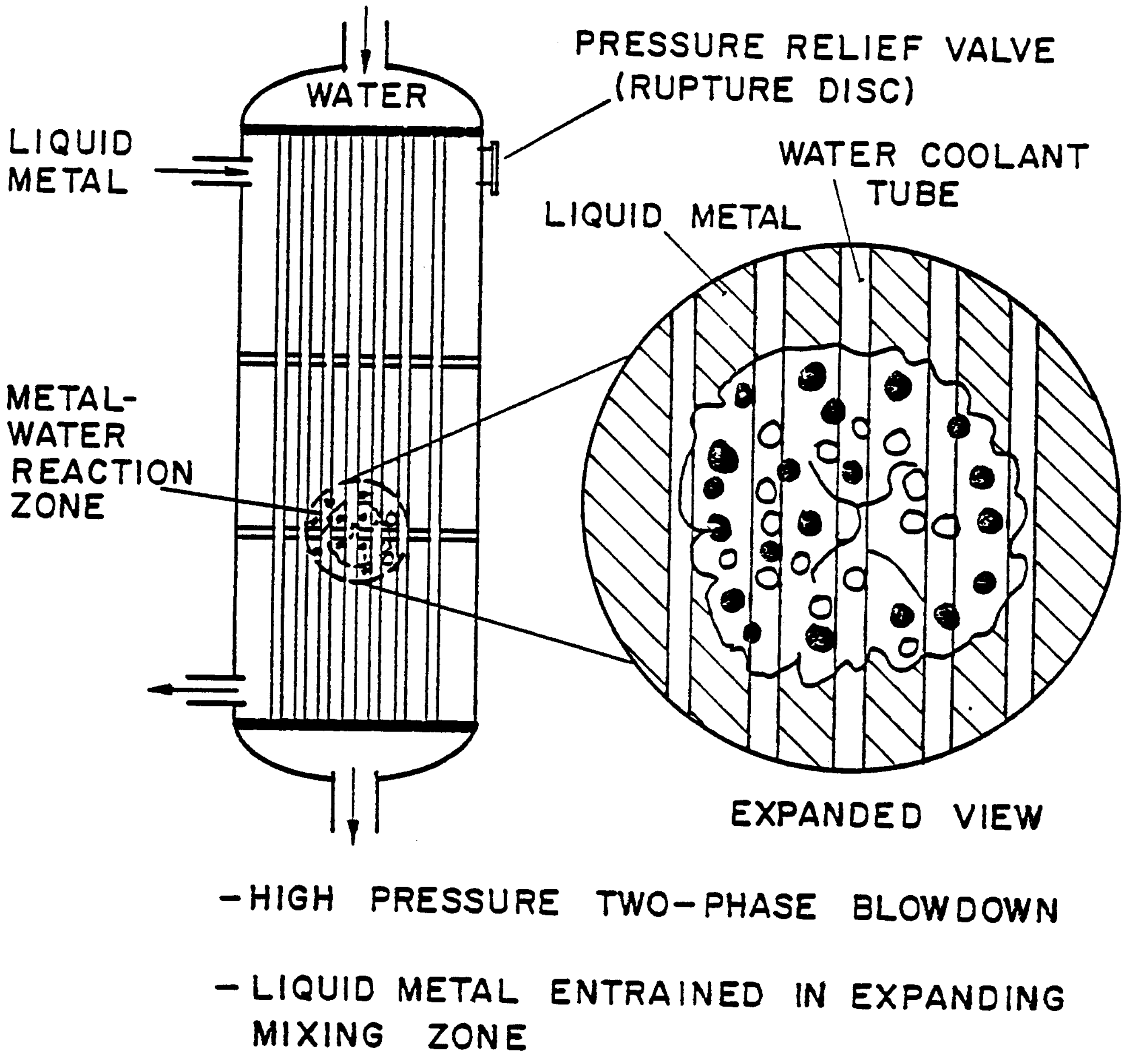

Fig. 2. Steam generator tube rupture.

- A spherical reaction zone of 10^{-5} m^3 exists immediately following the guillotine break of the tube. This provides an initial control volume for flow calculations and partially determines the initial energy associated with the pressure wave. This assumption is discussed more fully in the section devoted to loading on a steam tube.

The first two assumptions are conservative. If all of the water which escapes the steam tube is presumed to react immediately with lithium, the calculated generation of hydrogen will be at a maximum. A lack of back flow through the steam tube will result in a maximum flow rate of water into the lithium-lead. The remaining assumptions, though not necessarily conservative, are reasonable. They serve to simplify the physical picture so that the code can model the reaction one-dimensionally and use only two distinct zones (the reaction zone and a pure lithium-lead non-reaction zone).

The resultant time dependent pressure, temperature, and reaction zone radius (Figs. 3-5) provide the parameters for determining spatial temperature and pressure distributions during the first few milliseconds which follow the steam tube failure.

TEMPERATURE TRANSIENT

It has previously been determined that the temperature increase from the reaction of lithium-lead with water should not cause outright melting of the steam tubes [2]. However, degradation of the mechanical properties at high temperatures may warrant concern. The yield strength of HT-9 drops almost 500 MPa between 673 K (the lithium-lead temperature) and 1050 K (the reaction zone temperature).

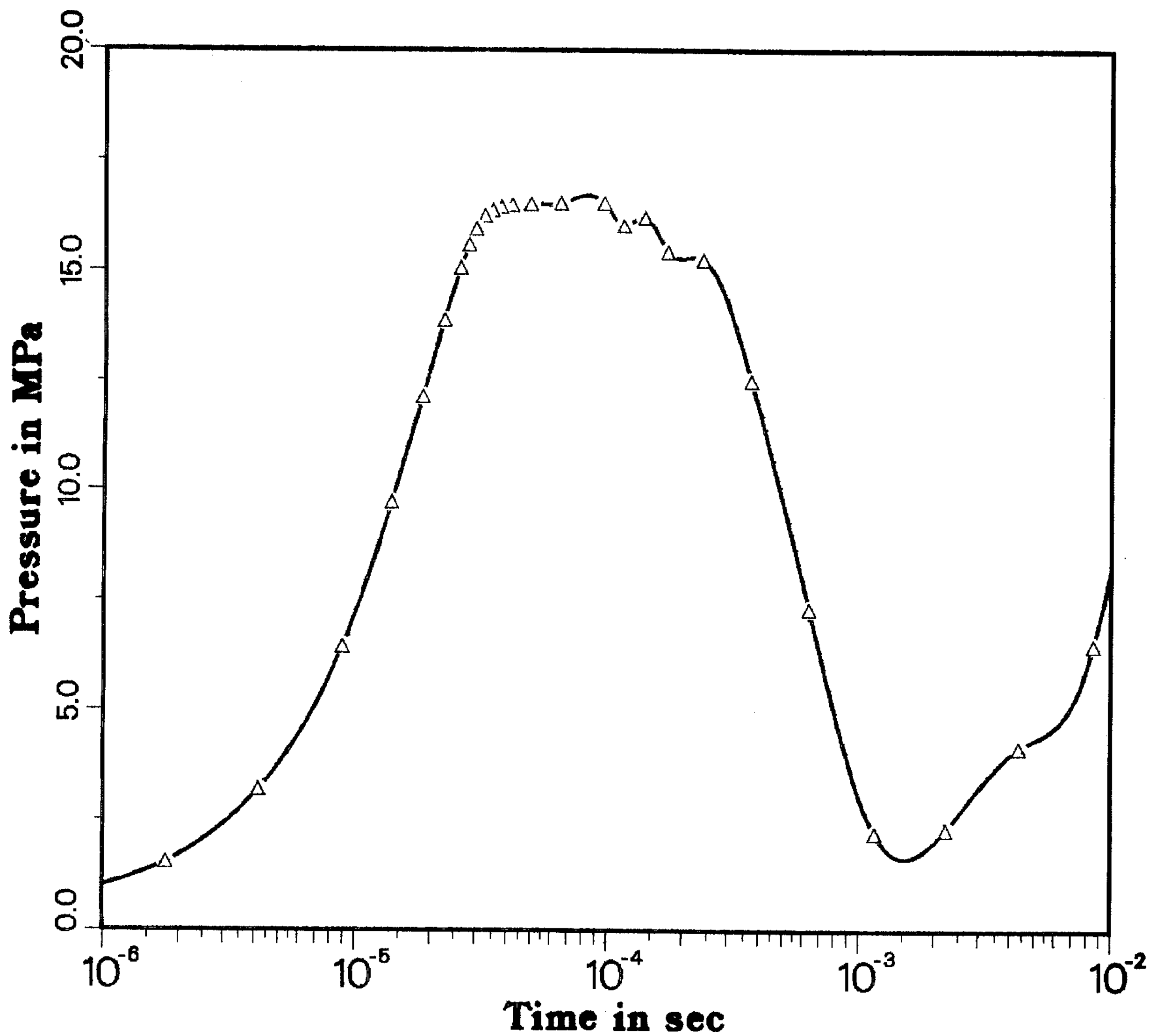

Fig. 3. Reaction zone pressure versus time.

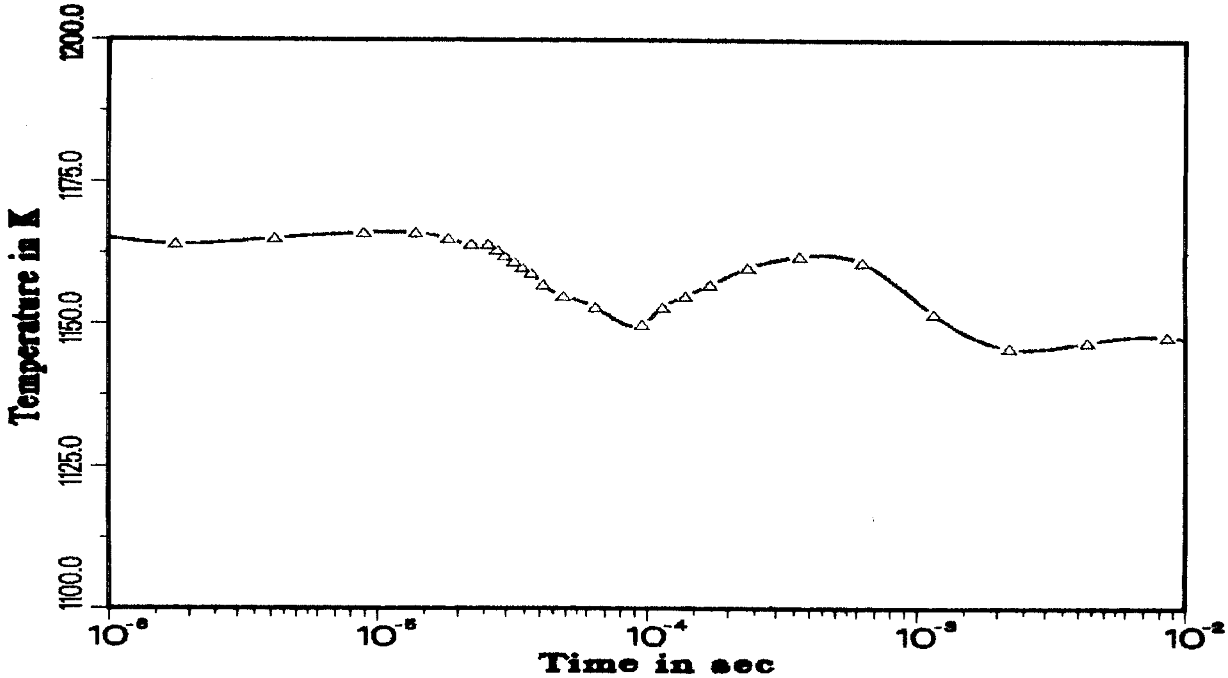

Fig. 4. Reaction zone temperature versus time.

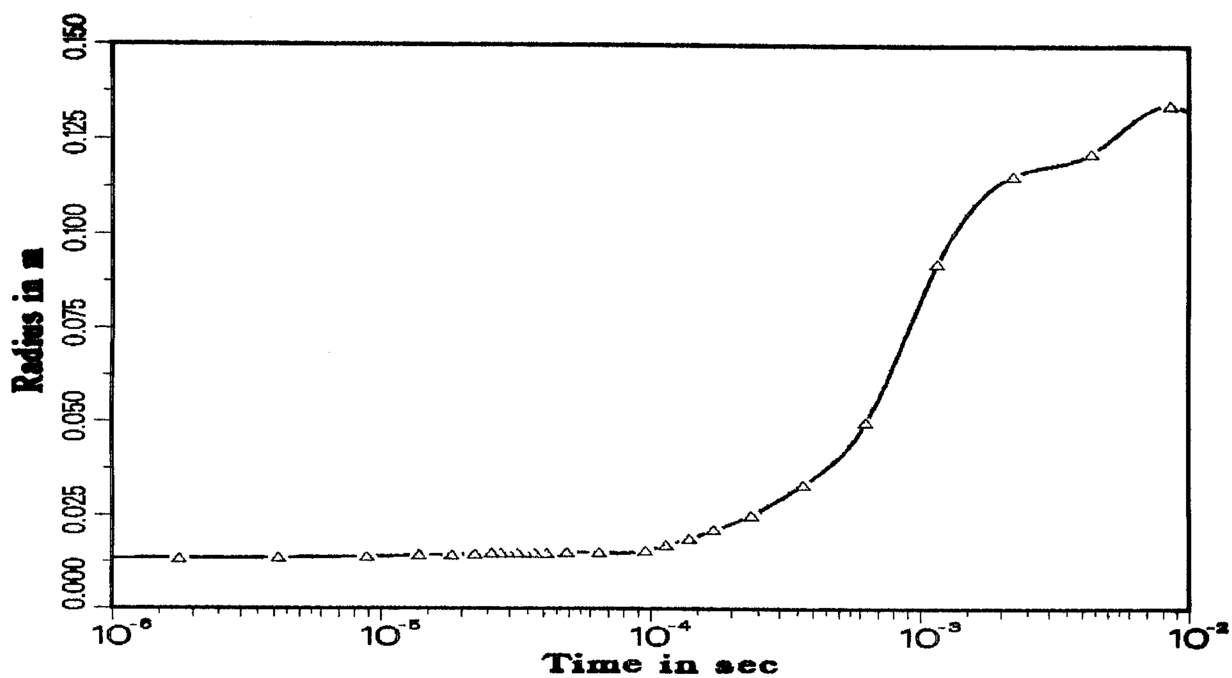

Fig. 5. Reaction zone radius versus time.

It is unnecessary to elevate the steam tube and generator outer shell temperatures for the pressure transient calculations due to the speed of the transient. The main pressure pulse occurs over a period of 1.5 ms. For the conduction of heat into the steam tubes and generator outer shell, this brief time interval produces a Fourier number on the order of 5×10^{-5}. This is too small for any appreciable heat transfer to occur during the main pressure transient.

After the main pressure transient has passed the steam tubes must still bear the shell to tube side pressure difference while at an elevated temperature. The change in the temperature of the steam tube over a period of many seconds or minutes is not clear. The time varying size, shape, and temperature of the reaction zone and the double-wall design of the tubes make it impractical to analytically determine the diminishing structural strength of the steam tube. To obtain an upper bound on the degradation of structural strength, the limiting case of an entire steam tube with the outside surface at the peak reaction zone temperature can be examined. Both the inner and outer walls are taken to be 2.0 mm thick. It was found that the gas gap between the tube walls (helium at 1.0 MPa was assumed) will keep the temperature of the entire outer tube within a few degrees of the reaction zone temperature. Most of the temperature drop between the reaction zone and the water takes place across the gap. Radiation heat transfer across the gap was not considered but inclusion of this should not vastly alter the average temperature of the outer tube and the following conclusions would remain unaltered.

It is necessary for the outer wall of the double-wall tube to bear only a portion of the total tube to shell side pressure difference. Information on the gas gap pressure was not available, thus a plot of tube outer wall stress versus pressure difference has been made (Fig. 6). Note that the abscissa is dimensionless and ranges from zero (entire pressure difference is across the inner wall) to one (all of the pressure difference is across the outer wall, about 17 MPa). Also shown is the yield stress of HT-9 at the reaction zone temperature of 1050 K. It can be seen that even when the entire outer wall is near the reaction zone temperature, it can bear most of the tube to shell side pressure difference. Though Fig. 6 suggests that the yield stress will not be exceeded, the safety margin is not clear. A more quantitative analysis requires additional information such as the mass flow rate, temperature, and quality of the water in the tube and more specifics on the design specifications of the duplex tube.

LOADING ON STEAM GENERATOR SHELL

The time dependent behavior of stresses on a dynamically loaded thin shell are not readily determined. Spatially asymmetric loadings are particularly difficult to model. Because of this, two limiting cases will be investigated. First, a symmetrical loading will be assumed so that analytical models for thin shells are applicable. Secondly, we assume a steam tube break near the edge of the tube array which produces a pressure distribution skewed towards one side of the steam generator. It is then possible to model the steam generator shell as a series of flat plates instead of a thin shell.

Symmetrical Case

Rather than considering the entire length of the steam generator, the shell is divided into a group of cylindrical sections. The ends of each section correspond to the grid spacers within the generator. It is presumed

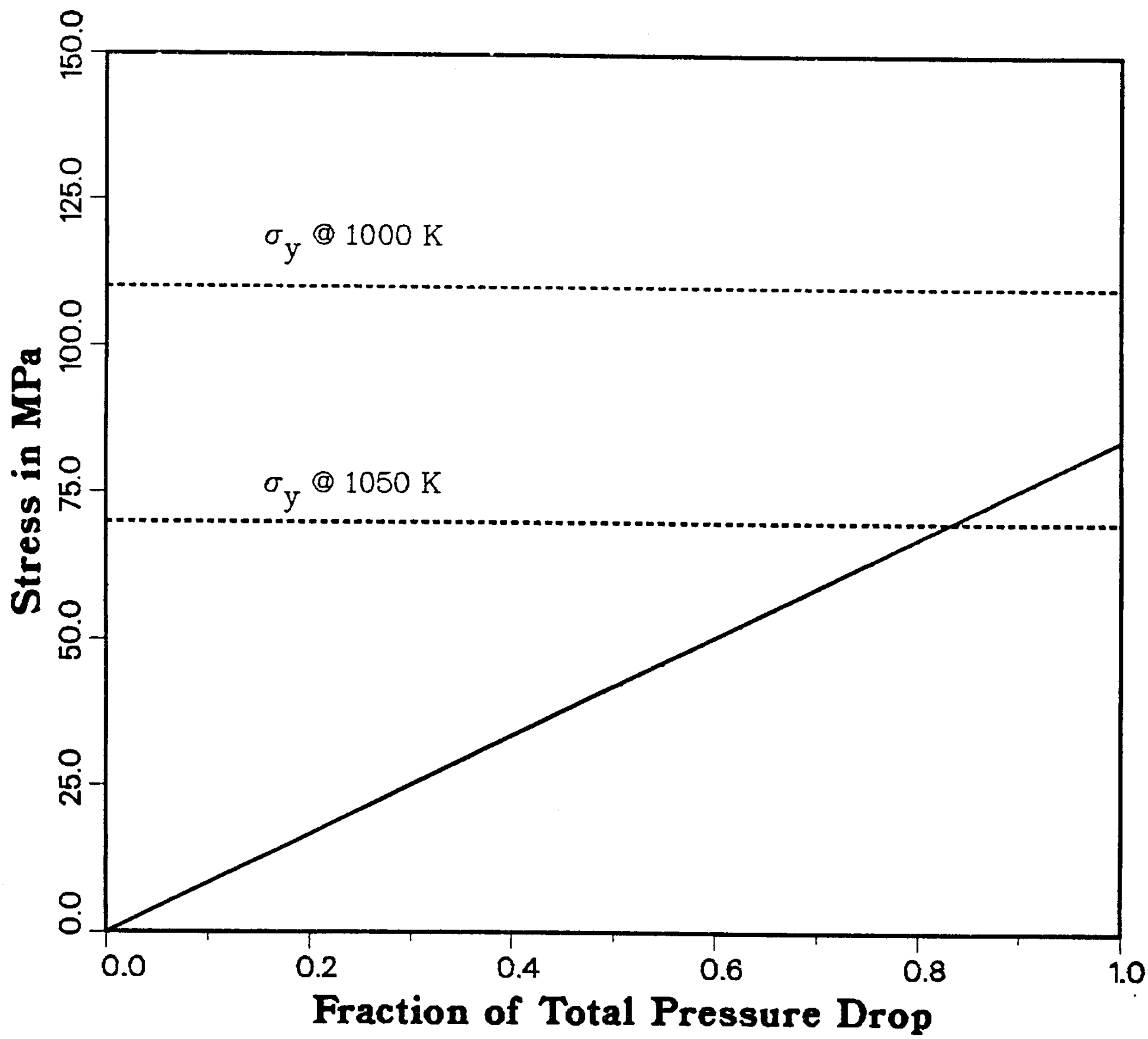

Fig. 6. Stress on steam tube outer wall versus fraction of total tube to shell side pressure drop.

that in addition to their function of supporting the steam tube array, the baffles restrict vibration of the shell where the two are joined (Fig. 1). Each cylinder, taken to be two meters long, is treated as an isolated structure with fixed edges. The height to diameter ratio is 0.89 which suggests that pressure waves originating near the center will arrive at all portions of the outer wall at approximately the same time. Having constructed this particular system, it will be possible to analytically determine the stresses on the shell as a function of time. To facilitate the stress calculations the following additional simplifications were necessary:

- The steam tubes do not reflect, decay, or retard the progress of the pressure wave. Effectively, the steam generator is filled with lithium-lead only. This is a conservative assumption. The steam tubes can be expected to attenuate the pressure wave as it travels towards the steam generator shell.
- Decay of the pressure wave is ~ 1/r, as if the wave retains a spherical shape as it propagates away from the break.
- The pressure impulse originates in the geometric center of the cylinder.
- Motion of the lithium-lead due to displacement by the expanding reaction zone does not contribute to forces on the shell.
- The pressure wave and resulting stresses are maximum in the cylinder of interest and are not considered for adjacent sections.

The longest natural period of the steam generator shell was found to be about ten times that of the pressure pulse when the lithium-lead is taken into account. If the lithium-lead is neglected, the longest natural period is reduced to 1.5 times that of the pressure pulse. From these two limits, we conclude that the pressure wave may be treated as an impulse loading. The expressions for stress on the shell do not include the period of the pulse, only total impulse. Possible changes in the structural strength of the shell due to the impact load are not considered.

Figures 7 and 8 represent the bending and circumferential stresses on the shell versus time for a shell thickness of 20 mm. In Fig. 9, the peak bending stress versus shell thickness is plotted. Stresses are determined by calculating the natural frequencies of vibration for the clamped cylindrical shell and summing the stresses associated with each mode of vibration [8]. The pertinent equations are:

$$\Omega_i^2 = \frac{D}{\rho h L^4}\left(\lambda_i^4 + \frac{EhL^4}{DR^2}\right)$$

$$D = \frac{Eh^3}{12(1-\nu^2)}$$

where

Ω_i = the natural frequency of vibration of the ith mode (s^{-1})

h = shell thickness (m)

R = shell radius (m)

L = shell length (m)

ρ = shell density (kg/m^3)

ν = Poisson's ratio

E = Young's modulus (N/m^2)

λ_i = eigenvalue for the ith mode of vibration.

The expressions used for calculation of the stresses are:

$$\sigma_x = \frac{EI_p}{2(1-r^2)\rho L^2} \sum_{i=1}^{n} \frac{4\lambda_i}{\Omega_i} \{M(\lambda_i) - \frac{N(\lambda_i)}{M(\lambda_i)} [T(\lambda_i) - 1]\} \sin \Omega_i t e^{-b\Omega_i t}$$

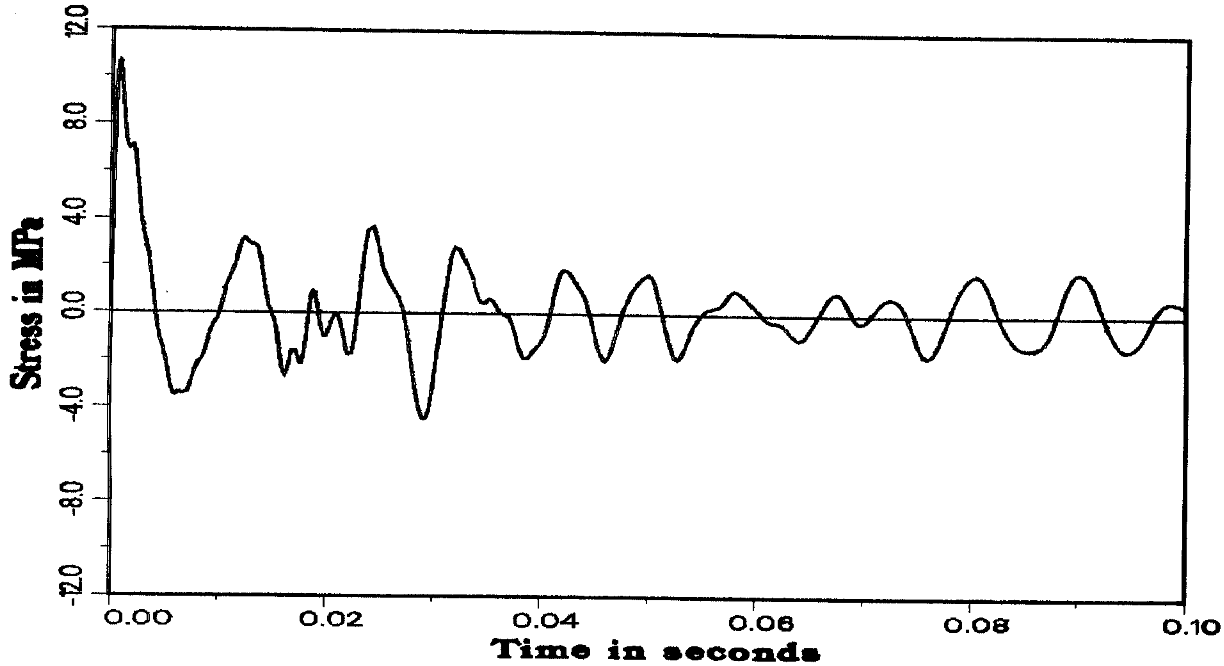

Fig. 7. Shell bending stress versus time.

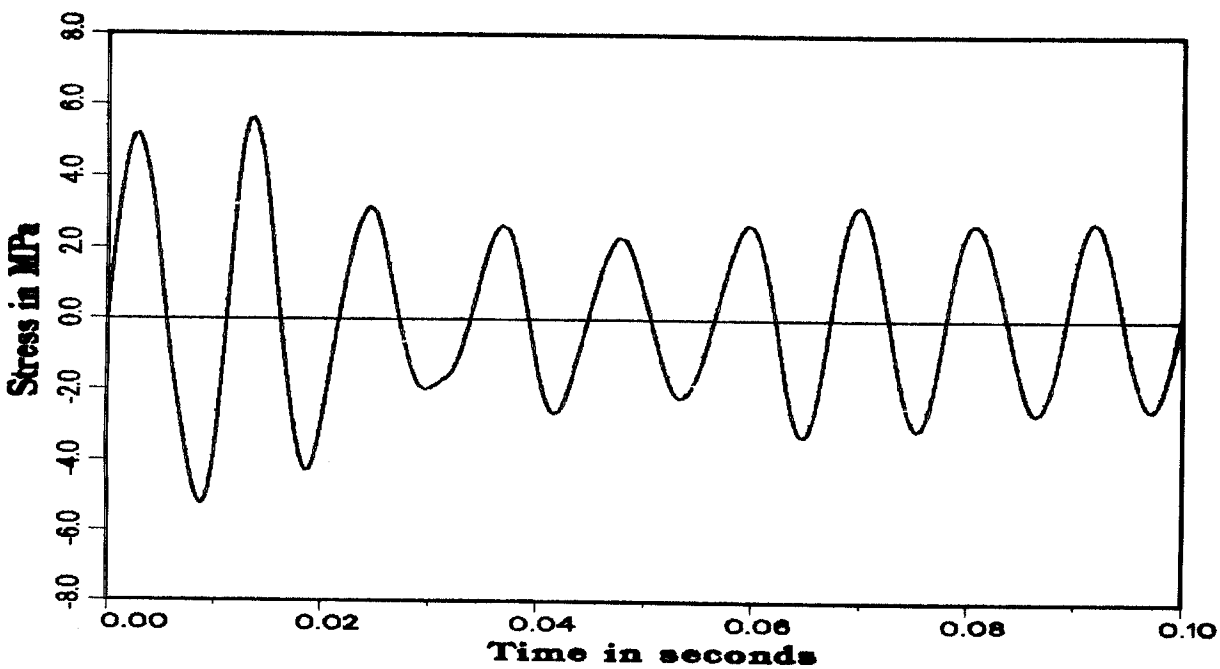

Fig. 8. Shell circumferential stress versus time.

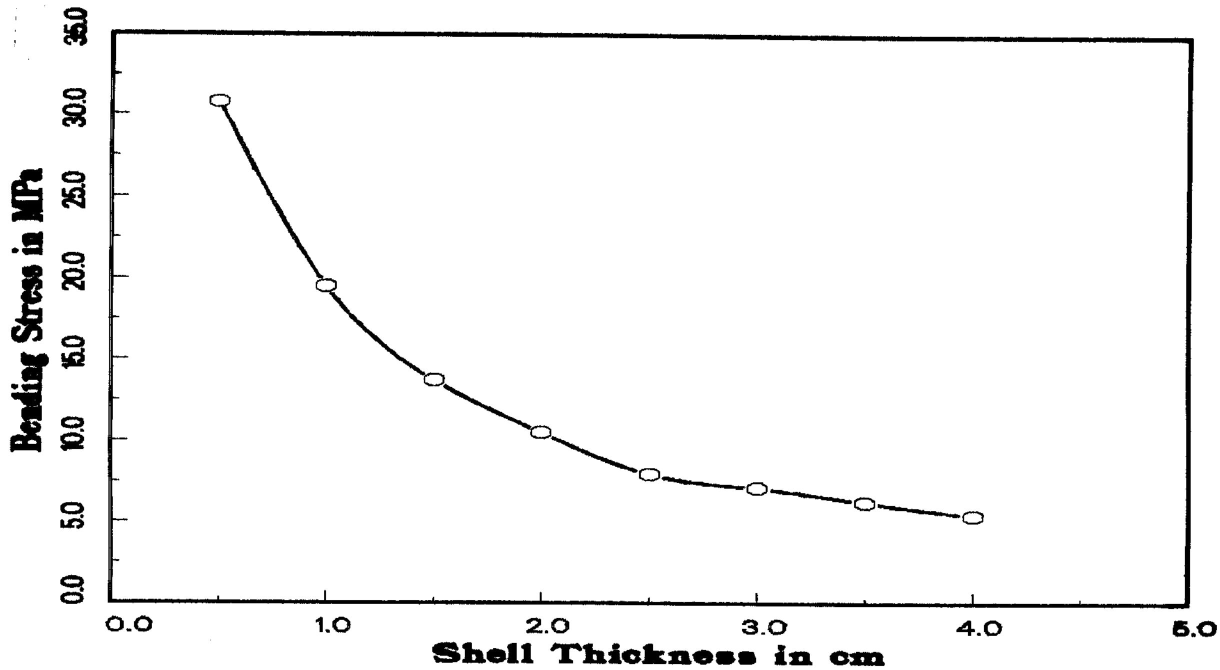

Fig. 9. Peak bending stress versus shell thickness.
Initial reaction zone radius is 13.4 mm.

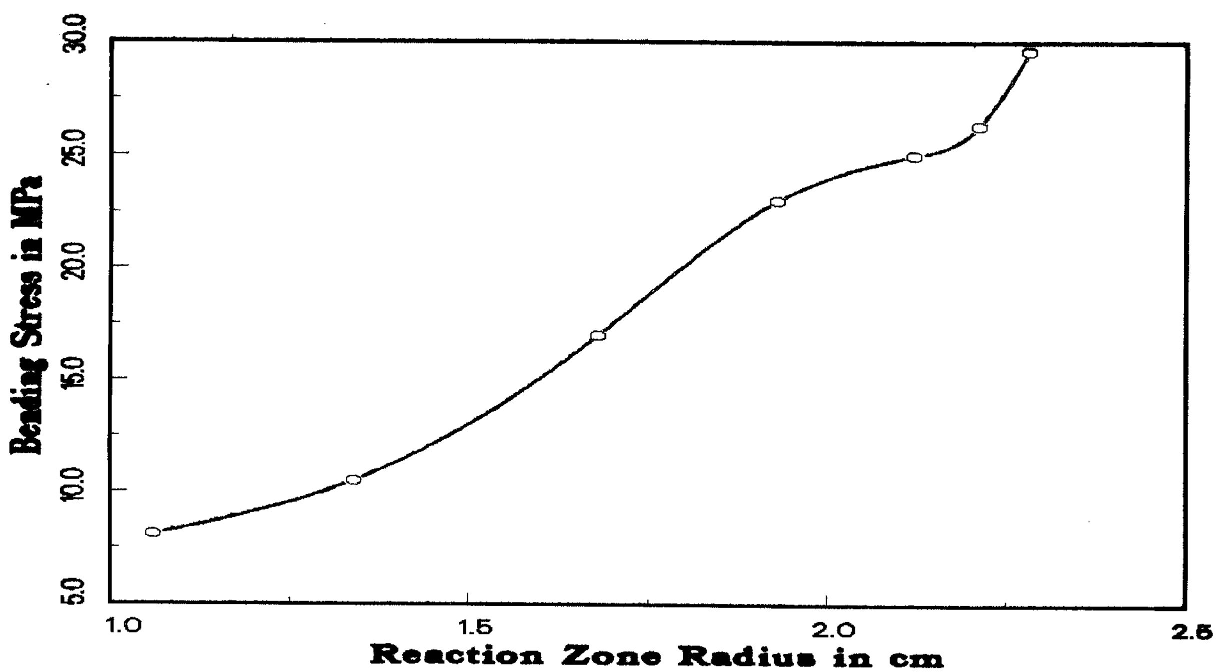

Fig. 10. Peak bending stress versus reaction zone radius.
Shell thickness is 20 mm.

$$\sigma_\theta = \frac{EI_p}{\rho hR} \sum_{i=1}^{n} \frac{4}{\lambda_i \Omega_i} \{N(\frac{\lambda_i}{2}) - \frac{N(\lambda_i)}{M(\lambda_i)} M(\frac{\lambda_i}{2})\}\{M(\lambda_i) - \frac{N(\lambda_i)}{M(\lambda_i)} [T(\lambda_i)-1]\} \sin \Omega_i te^{-b\Omega_i t}$$

where

$$M(\lambda_i) = \frac{1}{2} (\sinh \lambda_i - \sin \lambda_i)$$

$$N(\lambda_i) = \frac{1}{2} (\cosh \lambda_i - \cos \lambda_i)$$

$$T(\lambda_i) = \frac{1}{2} (\cosh \lambda_i + \cos \lambda_i)$$

σ_x = bending stress at x = 0, the clamped end (N/m^2)

σ_θ = hoop stress at x = L/2 (N/m^2)

I_p = impulse ($N\text{-}s/m^2$)

b = damping term (conservatively assumed to be 2%).

The lithium-lead in the steam generator must be accounted for by an added mass method which predicts an effective density for the shell [9]. This added mass method is of limited accuracy due in part to the complexity of the shell and fluid equations and because the steam generator is not a cylinder filled exclusively with lithium-lead. Neglecting the added mass effects of the lithium-lead would increase the peak shell stresses by a factor of five to ten. However, even for these increased stresses, there will still be a safety factor of at least two for generator wall thicknesses of 20 mm and greater. The minimum acceptable safety factor for the steam generator shell is not apparent but maintaining a safety factor of two despite extremely conservative assumptions strongly suggests that failure will not occur.

It has been indicated that the initial reaction zone size assumed by the MWI code (and which we cannot really know because it is a construct of the MWI model) affects the total energy associated with the pressure wave. This in turn affects the stresses on the structures. To observe this interdependence, peak generator shell bending stress versus initial reaction zone size is plotted in Fig. 10 for a shell thickness of 20 mm. Note that the initial reaction zone radius for the previous calculations is 13.4 mm.

For steam tube breaks near the center of the steam generator, the pressure pulse decays substantially before reaching the shell wall. In this case, peak stresses are expected to be well below typical yield stresses of high alloy steels. Instances where spatial decay of the pressure wave will not play such a dominant role must now be considered.

Asymmetrical Case

The most extreme case of an asymmetrical loading on the steam generator outer shell occurs after the rupture of a steam tube furthest (radially) from the center of the tube array. The major portion of the spherical wave moves away from the near wall allowing dispersion by the steam tubes and spatial decay to greatly reduce the peak pressure before making contact with the far walls. Only the fraction of the wave which moves towards the near wall and is within about 400. mm of the break is considered to contribute to mechanical stress on the outer shell. Due to the relatively small affected area, as compared to the area of the shell, the cylinder is treated as a system of several plates with a distributed, spatially constant, circular load applied at the center of one of the plates. The load is determined by integrating the spatially dependent pressure distribution over a circular section of the plate. The radius of the circle is limited to a distance at which the pulse pressure has decayed to less than 5% of the pressure at the circle's center.

The natural frequencies and stress are given by the following:

$$\Omega_i = \frac{\lambda_i}{b^2}\sqrt{\frac{D}{m}}$$

$$D = \frac{Eh^3}{12(1-\nu^2)}$$

$$\sigma_c = \frac{3W}{2\pi h^2}\left[(1+\nu)\ \ln\left(\frac{2b}{R}\right) + \beta_1\right] .$$

Where

m = Mass per area (kg/m^2)

W = Load (N)

R = Radius (m)

b = Width of the plate (m)

λ_i = A constant which is dependent upon the ratio of the length to the width of the plate and the mode of vibration.

β_1 = A constant, dependent upon the width to length ratio.

The stress calculated from the above expressions is multiplied by a dynamic load factor which accounts for the transient nature of the loading and allows the use of static stress models and failure criteria [10].

Figure 11 shows the peak stress on the steam generator shell versus shell thickness for 2 x 1 and 2 x 2 meter plates. Also, the yield strength of HT-9 at the bulk lithium lead temperature of 673 K is shown. It is not apparent what the plate size should be to adequately approximate the actual peak shell stress. The width of the plate affects the natural frequency of vibration

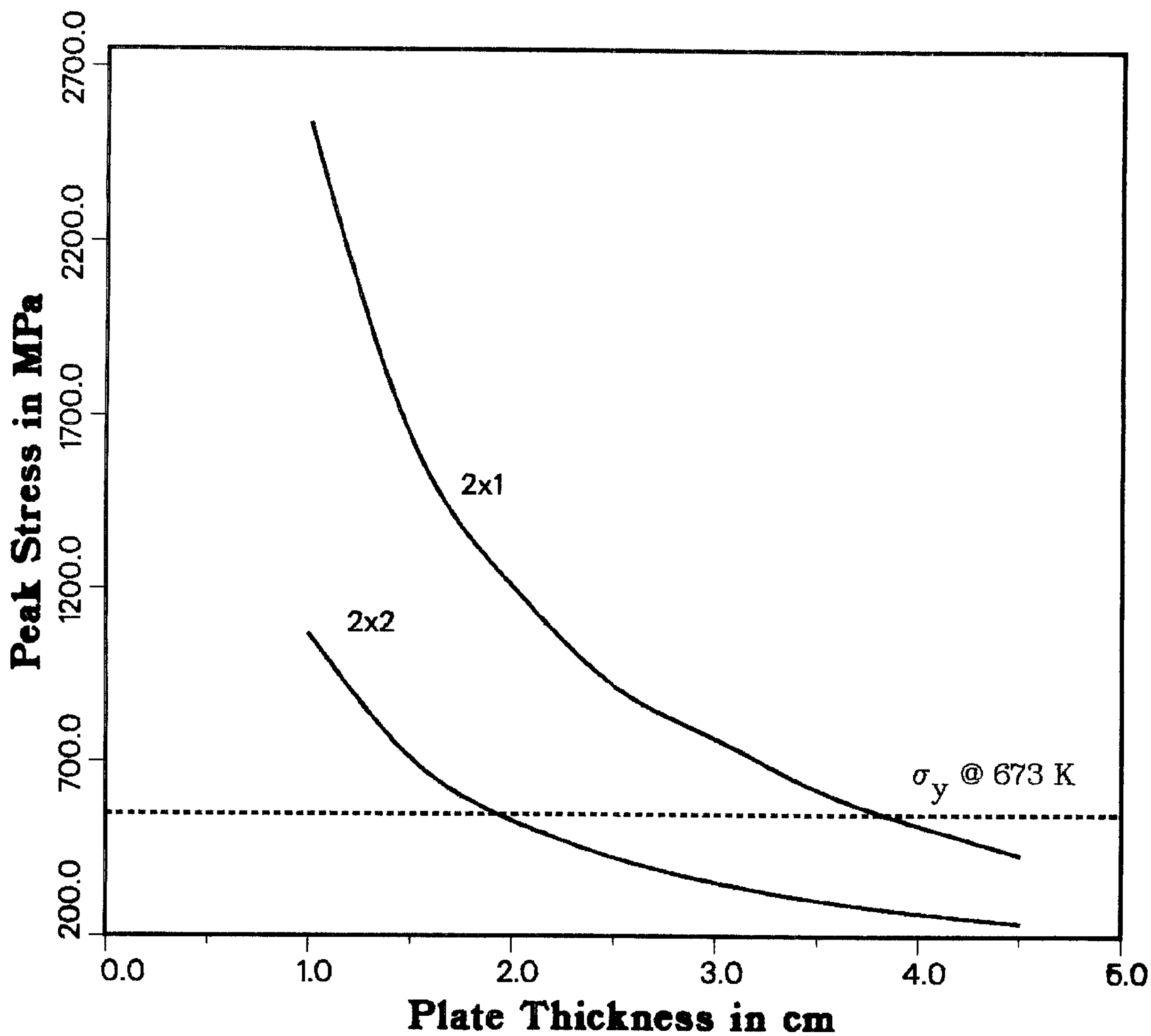

Fig. 11. Peak stress on plate versus plate thickness.

which in turn strongly determines the peak stress. Larger plates are a reasonable choice because they have natural frequencies comparable to the primary mode of the shell itself. However, if the asymmetrical loading causes higher modes of oscillation to become important, the smaller plates with higher frequencies of vibration may be more appropriate. Figure 11 indicates that, in either case, there will be appreciable stresses on the shell wall due to the magnitude of the pressure pulse and its proximity to the wall. The stresses increase with a reduction in plate size because the natural frequency of vibration is closer to the pulse frequency for the smaller plates.

LOADING ON A STEAM TUBE

The most serious scenario resulting from a steam tube rupture is the consequent failure of a second tube, presumably one adjacent to the initially breached tube, which produces a chain reaction of failures and leads to extensive damage of the steam generator. We wish to examine the effect of the pressure transient produced by a tube rupture upon neighboring steam tubes.

Calculation of the natural frequency of vibration of a double-wall tube would be quite complex. It is not clear how the inner and outer annuli will be coupled. Three fluids need to be considered for this analysis: lithium-lead against the outermost wall of the tube, fill gas between the tube walls, and water or steam for the innermost tube. One must also note that the grid spacers should serve as fixed supports for the outside wall but not the inside. There would be a different effective length for each of the tube walls. To eliminate these special considerations in determining vibrational frequencies and structural strength, the double-wall steam tube is treated as a single hollow cylinder (as if the inner and outer annuli were joined together). The effective length of the tube is regarded as two meters for the same reasons given for the steam generator outer shell. The effect of the lithium-lead upon the frequency of vibration of the tube was not treated here. This is conservative because the heavy fluid surrounding the steam tube will lower the frequency of vibration and reduce the dynamic load factor [10]. This, in turn, reduces the calculated stresses.

The effects of a spherical wave on a cylindrical tube are modeled two-dimensionally by alternatively considering a cylindrical wave on a flat beam. The pressure difference between the side of the beam facing towards the rupture and that which faces away results in a distributed load on the beam. The pressure difference is summed over the surface near the break for the duration of the pulse to obtain a resultant impulse on the beam. The natural period of vibration of the tube is roughly forty times the pressure pulse period which allows one to treat this as a square pulse that passes before the tube can react. The net total load upon the tube is adjusted with a dynamic load factor as was done with the case of the asymmetric loading on the steam generator shell.

The steam tube of interest is within 40 mm of the break and so the initial size of the reaction zone again becomes important. Figure 12 shows the peak stress on the tube versus the initial reaction zone radius. The bending stress remains below the yield stress for the given range of reaction zone radii and yet several uncertainties exist. These include the true natural frequency of the double-wall tube (filled with water and surrounded by lithium-lead), the net impulse on the tube, and a determination of the initial reaction zone volume. The lithium-lead and water which are in contact with the steam tube will tend to lower the natural frequency of oscillation of the

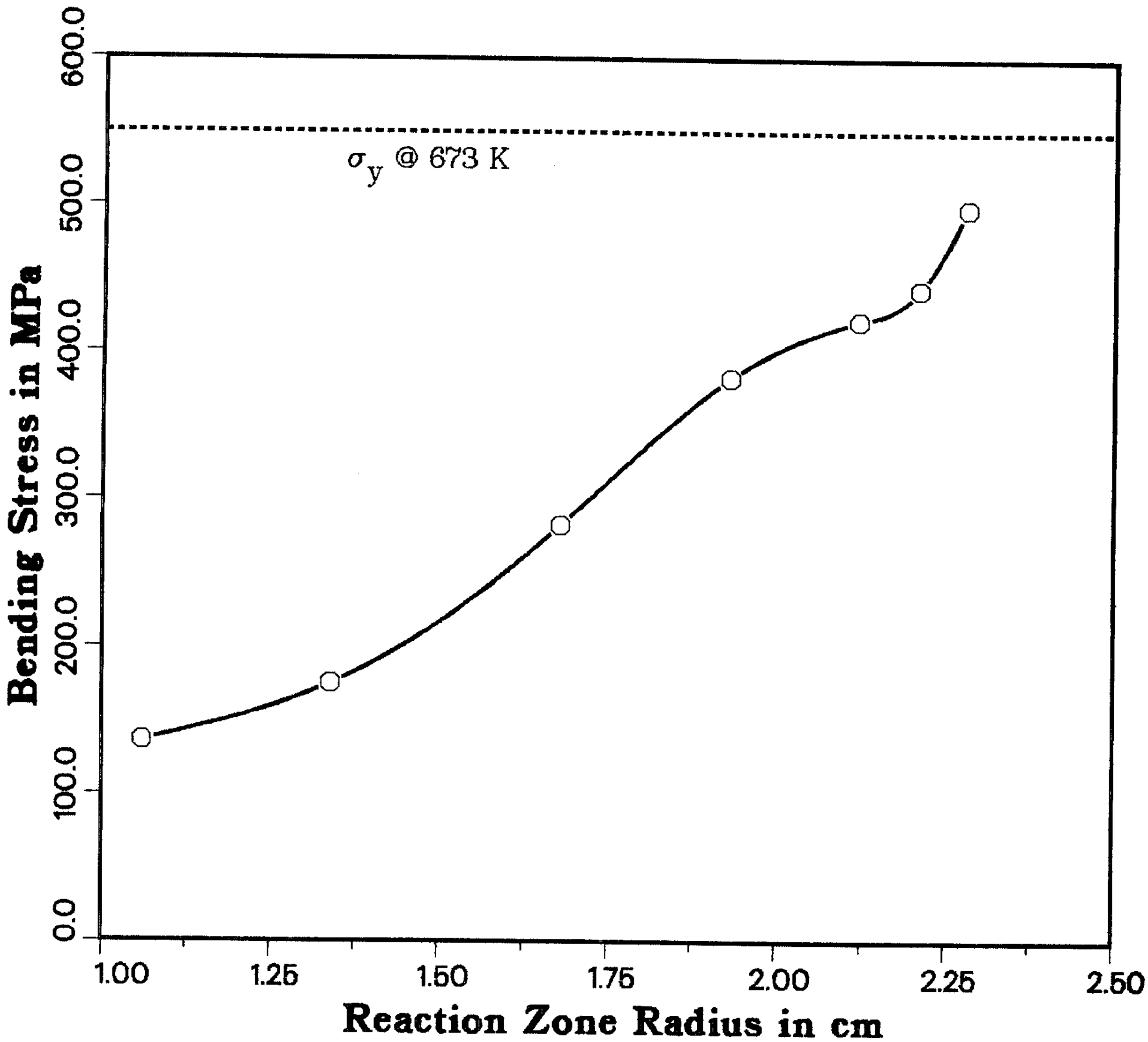

Fig. 12. Peak stress on the tube versus initial reaction zone radius.

tube. This results in a reduction of peak stress. Also, a portion of the pressure wave dissipates because, in reality, it propagates anisentropically. Pressure wave reflections may increase stresses by reducing the pressure on the 'back side' of the tube.

By far the largest variation in tube stress is produced by the uncertainty in initial reaction zone size. If the initial reaction zone radius is increased from 10 to 20 mm the tube stress jumps up by over 250 MPa. The size and pressure of the reaction zone, at early stages in the transient, greatly affect the resultant stress. A more sophisticated calculation is necessary to obtain better than order of magnitude estimations of stress on the steam tube.

ATHENA

The pressure history generated by the MWI code has provided the input parameters of pulse height, period, and total impulse for the steam generator stress calculation. This pressure history also shaped the simplifying assumptions made to aid these calculations. Reproducing the results of the MWI code with an alternative method would be useful in determining the accuracy of the previous assumptions and calculations. To accomplish this, a one-dimensional thermal hydraulics code named ATHENA (Advanced Thermal Hydraulic Energy Network Analyzer) was chosen.

A limitation in modelling the steam tube break with this code is ATHENA's inability to mix two different fluids such as water and lithium-lead. The effects of a chemical reaction between lithium and water, which results in the generation of energy, hydrogen gas, and other byproducts, will be lost. In addition, the interaction of high pressure water flashing into a volume surrounded by high density lithium-lead cannot be readily modelled.

The ATHENA model of the steam tube break consists of three interconnected pipes (Fig. 13). The first is a large, high pressure sink which is at the tube side pressure of 17.0 MPa. This connects to a short pipe segment (the cross-sectional area is twice that of a steam tube) and this empties into a low pressure sink of 0.17 MPa. Here, an important parameter is the low pressure pipe diameter. The smaller the pipe the higher the peak downstream pressure. The steam tubes surrounding the broken tube will serve to contain the pressure pulse suggesting that a low pressure sink the size of the steam generator would not be appropriate. Low pressure sink diameters of one and three times the steam tube lattice pitch are chosen to observe the variation in peak downstream pressure.

Since water and lithium-lead cannot be intermixed using ATHENA, the system was filled alternately with water and lithium-lead. Figures 14 and 15 show high pressure saturated water blowing down into low pressure water. Figures 16 and 17 are for the same system with lithium-lead replacing the water. The pressures are shown for distances of 23 and 230 mm downstream from the entrance to the low pressure sink. All four traces share the common trait of lacking the pressure 'pulse' that occurred with the MWI code. A quick ramp-up of the pressure to some steady value resulted in each case. With the ATHENA model, there is no reaction zone which fills with hydrogen, heats up, and quickly expands to cause a drop in pressure near the break.

For each fluid, the peak pressure always drops sharply when the low pressure sink radius is increased. This suggests that the extent to which the

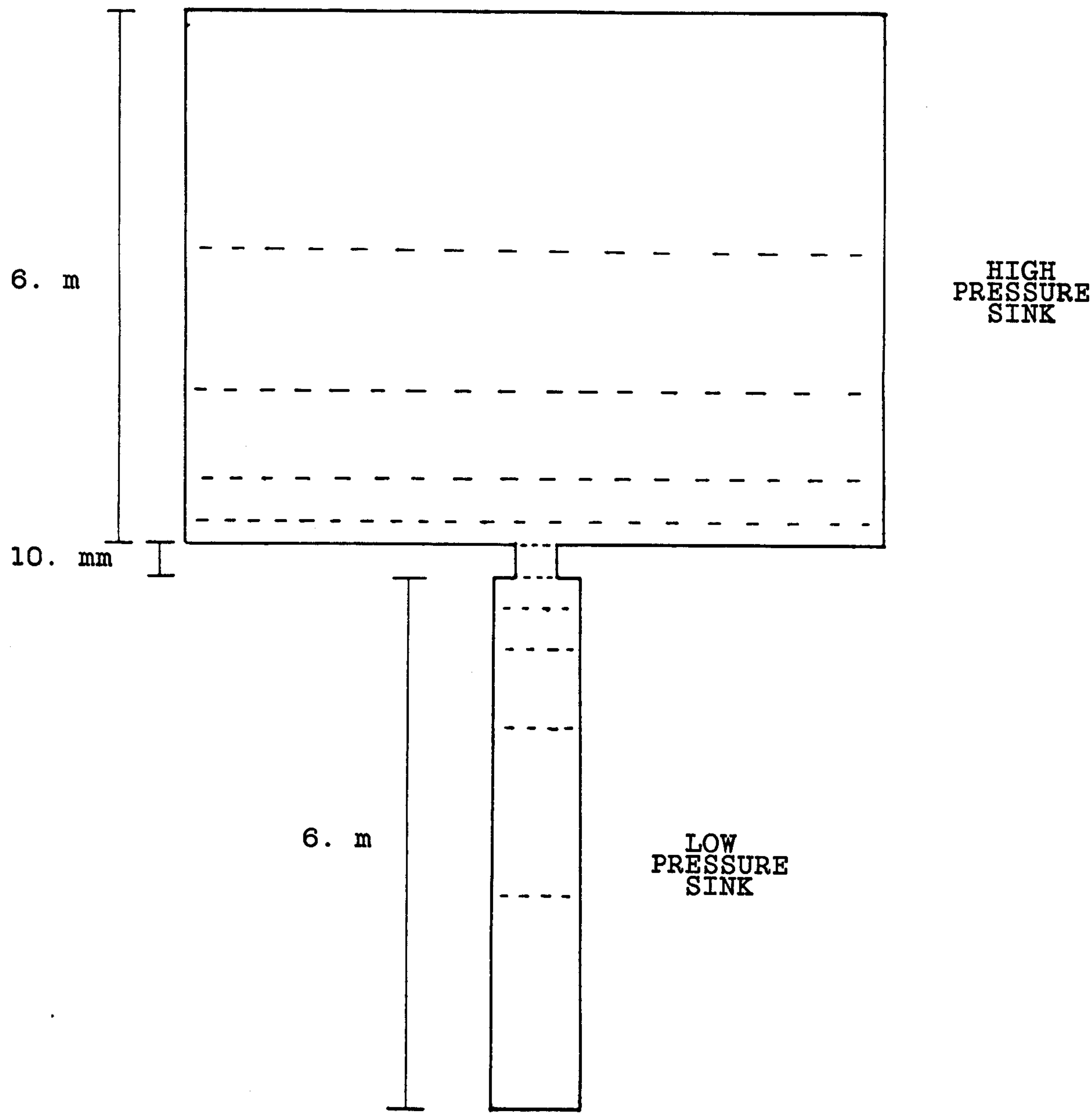

Fig. 13. Schematic of blowdown system for ATHENA. [Dotted lines represent changing control volume size and not the total number of volumes. There are a total of 99 control volumes in the system.]

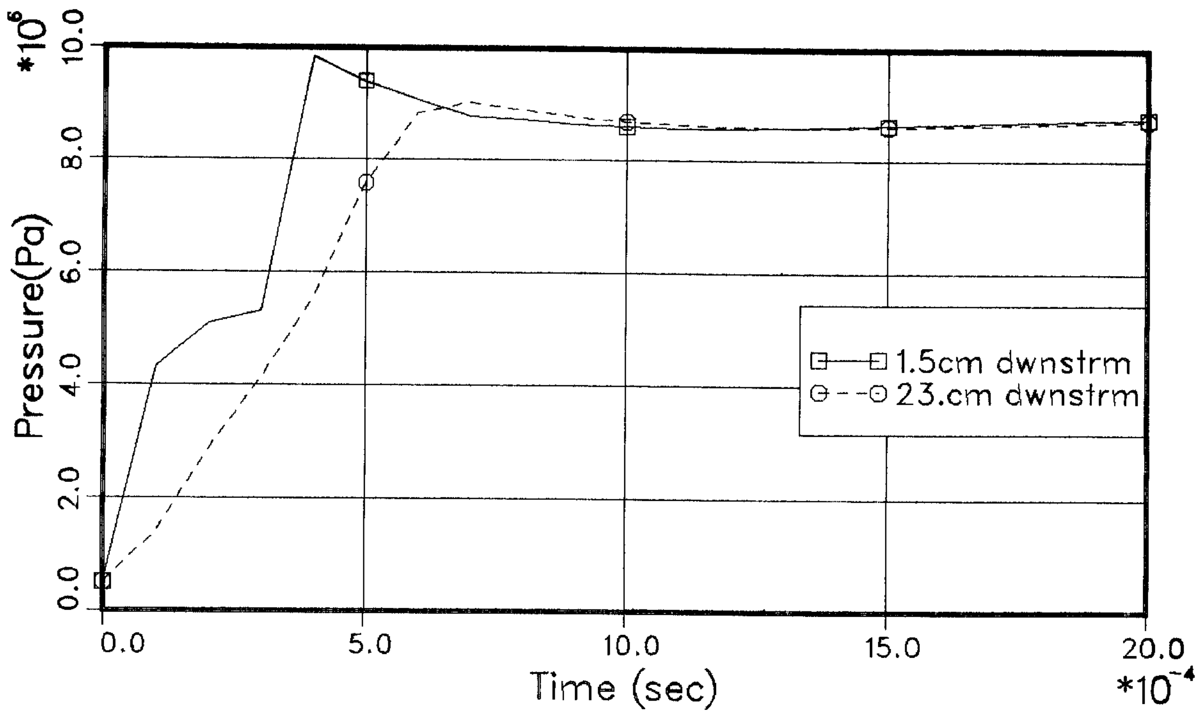

Fig. 14. Water pressure downstream of break for a low pressure sink diameter of 7.3 cm.

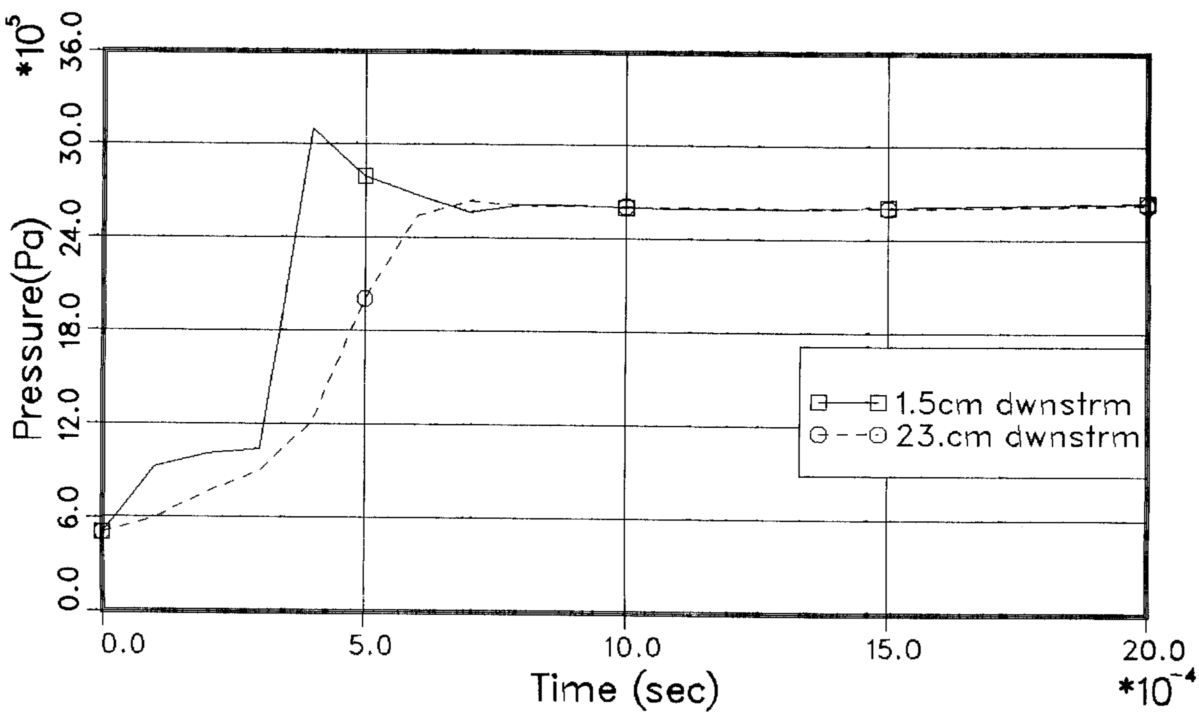

Fig. 15. Water pressure downstream of break for a low pressure sink diameter of 22 cm.

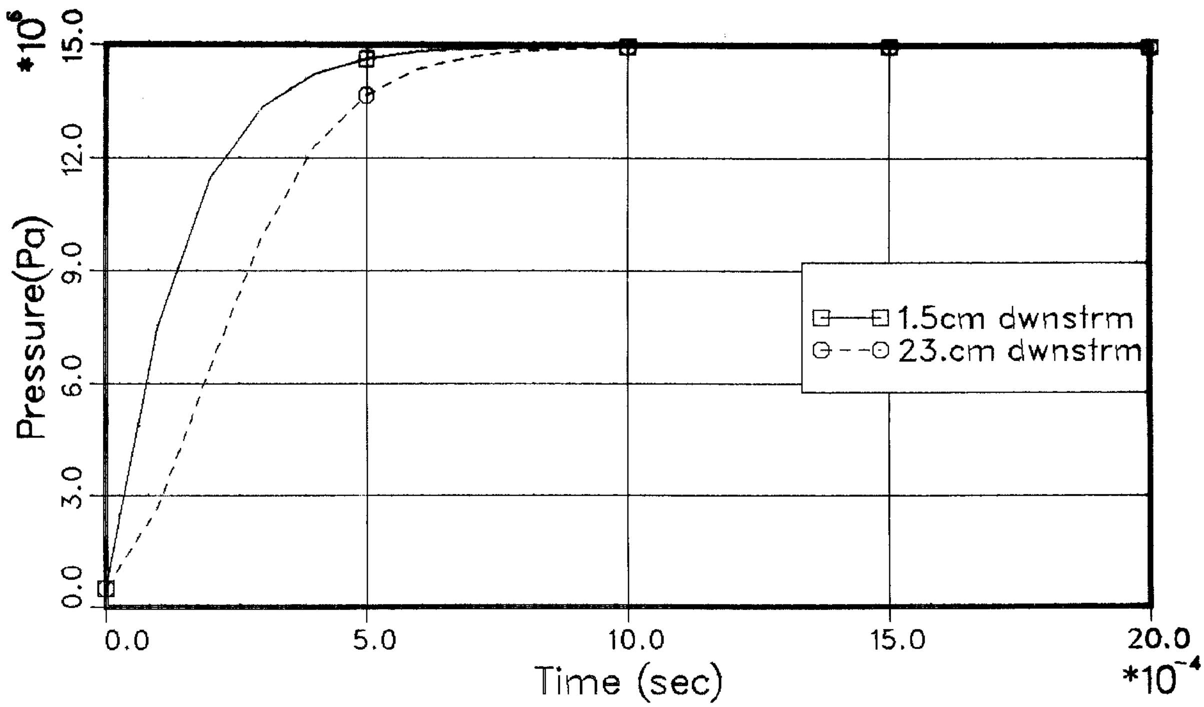

Fig. 16. Lithium-lead pressure downstream of break for a low pressure sink diameter of 7.3 cm.

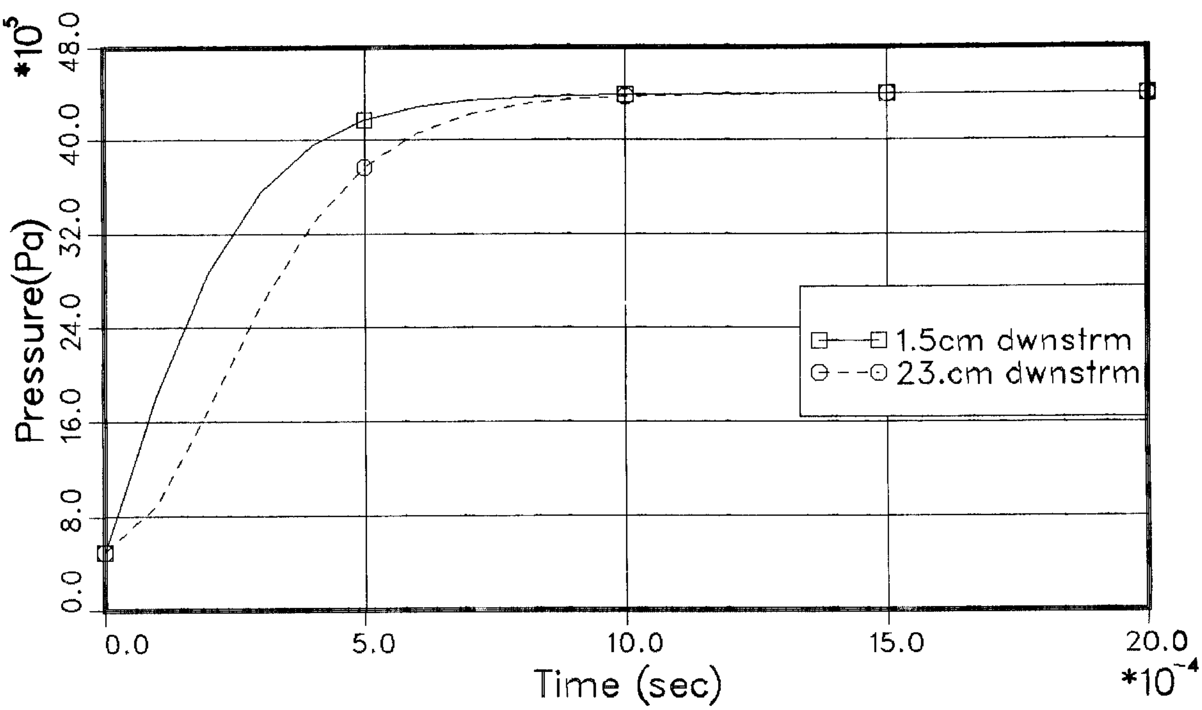

Fig. 17. Lithium-lead pressure downstream of break for a low pressure sink diameter of 22 cm.

surrounding steam tubes contain the pressure transient may prove to be important in determining component stresses.

Spatial decay of the pressure jump could have been added to the ATHENA model by increasing the cross sectional area of the low pressure pipe control volumes with increasing distance downstream. This, however, would not alter the basic pulse shape at any one point in the low pressure sink.

DISCUSSION AND OBSERVATIONS

The MWI and ATHENA codes provide two substantially different versions of the steam tube break scenario. ATHENA essentially gives a blowdown through a steam tube into a low pressure vessel. Mixing of lithium-lead with water was not allowed and so the elevated temperature and hydrogen gas buildup near the break were not accounted for. The lithium-water reaction is violent enough that it is doubtful if one can neglect this and still obtain the proper pulse shape and/or magnitude. One might consider adding portions of the MWI code to ATHENA. If this is to be undertaken, three basic changes must be implemented:

- ATHENA must simulate the mixing of two immiscible dissimilar liquids (i.e. lithium-lead and water).
- Hydrogen production must be included in the form of a noncondensible gas.
- One would have to account for the generation of heat from the lithium-water reaction.

Large difficulties will be encountered due to the nature of ATHENA's fluid flow and heat transfer models. Thus a radical change would be necessary for MWI models to be incorporated into ATHENA.

The pressure pulse produced by the MWI code proves to be quite large (likely conservative) and in some cases may result in unacceptable loadings on some steam generator components. In particular, the tube break near the steam generator wall was seen as the worst case. The close proximity of the tube to the wall prevented the pulse from decaying sufficiently to produce moderate loadings. The detailed behavior of the pressure pulse and the structural response of the steam generator to highly asymmetric loadings must be more accurately determined to ensure that yield stresses are not exceeded.

It has been suggested [11] that stresses between the tube sheet and the steam tube may merit concern. In the analysis of loading on a steam tube, the tube ends were assumed to be fixed. However, there is the possibility of failure due to 'impact fretting'. The impact loading produces small lateral displacements at the juncture of the steam tube and tube sheet [12]. Treatment of this would require detailed evaluation of the initial conditions at the tube ends. If the joint allows vibrational motion, inertial effects of the lithium-lead may be important. Though impact fretting and effects of a similar nature may be of concern, they are beyond the scope of this report.

It was observed that varying the initial radius of the reaction zone in the MWI code had an appreciable effect upon peak structural stresses. The initial flow rates and mixing parameters early in the transient can have a great effect upon the pressure and temperature history of the transient. Even the apparently simple assumption of a guillotine break is complicated by initial conditions which are not readily determined. The radius of 10-20 mm for the initial reaction zone radius is consistent with this conservative assumption.

Several conservative assumptions were made during the course of the analysis. The assumptions of a complete, instantaneous guillotine break and the complete reaction of water with lithium are certainly the most severe. The guillotine break is rather unrealistic, especially for a double-walled steam tube. Any relaxation of these assumptions would significantly reduce the calculated component stresses.

In summary, if one accepts the MWI model as a reasonable description of the guillotine break scenario, we find that tube ruptures near the steam generator shell should be the only serious concern. Spatial decay of the pressure wave dominates all other cases so that the wave dissipates without permanent damage to neighboring components. Also, the elevated temperatures which result from the lithium-water reaction should not prompt the failure of steam tubes, during the initial pressure transient. After the transient, a portion of the steam tube outer wall may heat up to the reaction zone temperature, reducing the yield strength considerably. This will produce difficulties only if the outer wall must bear most of the tube to shell side pressure drop.

ACKNOWLEDGEMENT

Support for this work has been provided by the U.S. Department of Energy through the EG&G fusion safety program. Great thanks to Prof. Roxann Engelstad for her invaluable help.

REFERENCES

[1] S.J. Piet et al., "Liquid Metal Chemical Reaction Safety in Fusion Facilities," Fusion Engineering and Design, 5, North-Holland, Amsterdam, 1987.

[2] J.P. Herzog and M.L. Corradini, "Modelling of Lithium-Lead/Water Interactions in a Fusion Reactor Design," University of Wisconsin, UWFDM-559, (August 1984).

[3] J.P. Herzog and M.L. Corradini, "Modelling of Lithium-Lead/Water Interactions in a Fusion Reactor Design-Part 2: Modelling Improvements," University of Wisconsin, UWFDM-649 (September 1985).

[4] H. Chow, P.A. Roth, K.E. Carlson and V.H. Ransom, "ATHENA Code Manual", Vol. 1 Draft, EG&G Idaho Report RST-7034, (September 1985).

[5] V.H. Ransom et al., RELAP5/MOD2 Code Manual, NUREG/CR-4312, EGG-2396, August 1985, all volumes.

[6] Presentation by Westinghouse of Pensacola, Florida at MARS (Mirror Advanced Reactor Study) meeting at TRW in Los Angeles, CA, April 1983.

[7] In Ref. 2, Fig. 1, p. 4.

[8] E.G. Lovell and R.L. Engelstad, "Dynamic Stress Analysis of Light Ion Fusion Target Development Facility Reaction Chamber," Nuclear Technology/Fusion, Vol. 4, pp. 878-882, September 1983.

[9] R.D. Blevins, Formulas for Natural Frequency and Mode Shape, 1979, New York: Van Nostrand Reinhold Co.

[10] Corps of Engineers, Department of the Army, "Design of Structures to Resist the Effects of Atomic Weapons/Principles of Dynamic Analysis and Design," EM 1110-345-415, 15 March 1957.

[11] S.J. Piet and L.C. Cadwallader, EG&G Idaho, Inc., Private Communication (January 1988).

[12] J.A. Collins, Failure of Materials in Mechanical Design: Analysis, Prediction, Prevention, New York: John Wiley and Sons, Inc., 1981.

[13] M.D. Mikhailov, Unified Analysis and Solutions of Heat and Mass Diffusion, 1984, New York: John Wiley and Sons, Inc.

[14] R. Szilard, Theory and Analysis of Plates, 1974, Englewood Cliffs, NJ: Prentice-Hall Inc.

[15] R.J. Roark and W.C. Young, Formulas for Stress and Strain, 1975, New York: McGraw-Hill Book Company.

[16] E. Skudrzyk, Simple and Complex Vibratory Systems, 1968, University Park: The Pennsylvania State University Press.

[17] R. Bird et al., Transport Phenomena, New York: John Wiley and Sons, Inc., 1960.

[18] M.M. El-Wakil, Nuclear Heat Transport, Illinois: The American Nuclear Society, 1978.